

## Upward Monocular Camera based SLAM Using Corner and Door Features

Seo-Yeon Hwang, Jae-Bok Song

*Dept. of Mechanical Eng., Korea University, Seoul, Korea  
(Tel: 82-2-3290-3363; e-mail: etoile02, jbsong@korea.ac.kr)*

---

**Abstract:** Small-size robots usually employ cheap sensors for navigation instead of expensive laser scanners or stereo cameras. This paper deals with the SLAM process using a monocular camera which heads upward to see the ceiling and the upper portion of a wall. This upward camera has some advantages of being free of dynamic obstacles, the fixed distance to the ceiling and so on. Most past research based on an upward camera used corner features for localization, which are not always extracted in an indoor environment. In this research, however, door features are added to overcome this difficulty involved in SLAM using the corner features only. A door helps not only to estimate the pose of a robot, but also to divide the environment into several meaningful areas. A particle filter is adopted to estimate the door position to check whether the specific door is suitable for the SLAM process before registering it in the EKF algorithm. Experimental results show that the proposed scheme works successfully in various indoor environments.

---

### 1. INTRODUCTION

When a robot navigates in an unknown environment, both accurate pose estimation of the robot and map building of the environment are important issues. Therefore, SLAM (Simultaneous Localization And Mapping) becomes one of the most fundamental and challenging issues in the field of mobile robotics. A range sensor (i.e., laser scanners, sonar sensors, and IR scanners) and a vision sensor (i.e., monocular and stereo cameras) can be usually exploited for SLAM. A range sensor provides the range information directly, which makes feature extraction easier than a vision sensor. However, the features that can be extracted using the range information are limited to lines and corners. On the other hand, a vision sensor can provide much more information than a range sensor, but requires complicated image processing to extract invariant features.

Recently, small-size and/or relatively cheap robots such as robot vacuum cleaners have spread to our life. They, however, usually employ sonars or IR sensors as a range sensor, and these sensors provide relatively inaccurate range information which is not suitable for localization. Therefore, a vision sensor is considered a more important sensor. However, stereo cameras which can provide the range information as well are not frequently used for their high cost. Instead, in recent years, even the small-size robots have been equipped with low-cost monocular cameras.

Several approaches to SLAM have been proposed using a monocular camera. Davison achieved real-time 3D monocular SLAM with a wearable camera successfully (A. Davison, 2003, P. Smith et al., 2006). For a mobile robot, a forward camera is used to extract the corner or SIFT features, while a downward camera to obtain the line features between the wall and the floor in an indoor environment. On the other hand, an

upward camera can extract corner and line features for SLAM (J. Folkesson et al., 2005, W. Y. Jeong et al., 2006).

The scheme based on an upward camera has some advantages compared to other schemes. First, it is little affected by dynamic obstacles such as moving people since the camera sees the ceiling. Second, there is no scale and affine changes of a feature between successive ceiling images. Therefore, under these conditions, corner features have been extracted from the image as a main feature since it provides the robust matching results. However, the corner feature is not always extracted in various environments. Recently, much research has attempted to fuse different types of features such as the lines in addition to the corners. In this case, a disadvantage of one feature can be compensated by others.

The corner needs a complicated process to match, but it provides a reliable matching result since it uses an image patch around the corner. The line is easily distracted by nearby edges since there is no appropriate descriptor for line matching, but it is invariant to changes in illumination, distance, and viewpoint. Also, the line involves the information to divide the environment into the meaningful areas (P. Smith et al., 2006). Thus, fusing various types of features makes navigation stable in various environments.

To cope with the above problems, we propose a door extraction scheme for the monocular SLAM using an upward camera. In general, a door has common evidences; two vertical columns and one horizontal bar. All possible candidates for a door are generated based on these evidences from the image that has many lines extracted from the real environment, and the candidates are determined whether it is open or not. The extracted door feature is exploited to estimate the robot pose in the EKF (Extended Kalman Filter) SLAM with the corner feature and to divide the environment into the meaningful areas.

To use a feature such as a corner and a door in the EKF, reliable matching is very important. The corner is matched with the image patches by various methods such as NSSD (Normalized Sum of Squared Differences), representative gradients, and so on. However, line matching is one of the most difficult issues in the image processing field since a line has the insufficient surrounding information. In this research, the lines extracted from a door are reliable in matching since the door feature is matched only when the three evidences (two vertical columns and one horizontal bar) are collected simultaneously.

The remainder of this paper is organized as follows. Section 2 presents the basic concept of the monocular SLAM and the application procedure of EKF (Extended Kalman Filter) with corners. Section 3 presents the procedure of extracting candidates from the image. Section 4 describes how to determine whether the door candidate is open or not. Finally, section 5 and 6 present experimental results and conclusions.

## 2. EKF-BASED SLAM

A stereo camera directly provides the positions of the features in the image, but a monocular camera cannot provide such information at the stationary state. Thus, when the monocular camera is used as a main sensor to estimate the robot pose, the features should be observed at different positions to reduce the uncertainty of the position, as shown in Fig. 1. The first bearing information forms the possible area of the feature with the uncertainty shown in Fig. 1(a), and another bearing information is incorporated to reduce the uncertainty of the feature position, as shown in Fig. 1(b). Fig. 2 shows the reduction of the uncertainty of corner features which are extracted from the upward camera during SLAM in the real environment. In this paper, the EKF is adopted to deal with the relationship between the robot and features using a monocular camera.

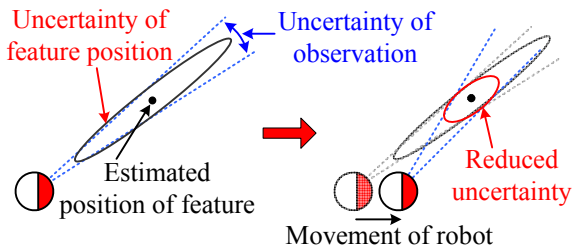


Fig. 1. Basic concept of monocular SLAM.

The EKF algorithm is usually adopted to handle nonlinearities involved in the robot motion. Since the corner and door features are used as landmarks in this research, the state vector and covariance matrix are defined as follows:

$$\mathbf{X} = [\mathbf{X}_R^T, \mathbf{X}_{C_1}^T, \dots, \mathbf{X}_{C_n}^T, \mathbf{X}_{D_1}^T, \dots, \mathbf{X}_{D_m}^T]^T \quad (1)$$

$$\mathbf{P} = \begin{bmatrix} \mathbf{P}_R & \mathbf{P}_{RC} & \mathbf{P}_{RD} \\ \mathbf{P}_{CR} & \mathbf{P}_C & \mathbf{P}_{CD} \\ \mathbf{P}_{DR} & \mathbf{P}_{DC} & \mathbf{P}_D \end{bmatrix} \quad (2)$$

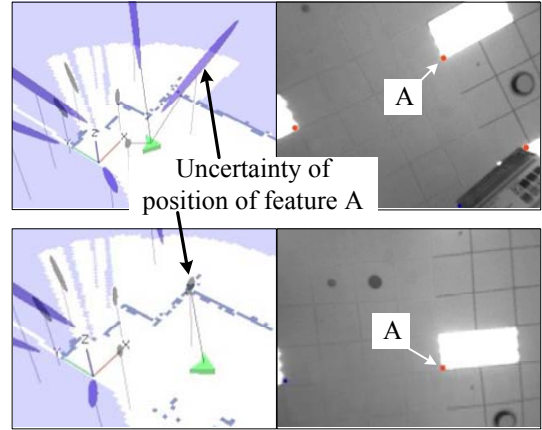


Fig. 2. Reduction in uncertainty (ellipsoid) of the corner feature during robot motion.

where  $\mathbf{X}_R = [r_x, r_y, r_\theta]^T$  represents the position ( $r_x$  and  $r_y$ ) and the orientation ( $r_\theta$ ) of the robot,  $\mathbf{X}_{C_i} = [c_x, c_y, c_z]^T$  is the position of the  $i$ -th corner where  $c_x$ ,  $c_y$ , and  $c_z$  are its  $x$ ,  $y$ , and  $z$  coordinates.  $\mathbf{X}_{D_j} = [c_{1x}, c_{1y}, c_{2x}, c_{2y}]^T$  represents the  $j$ -th door which is defined by two vertical columns,  $c_1$  and  $c_2$  in the  $x$ - $y$  plane. All variables are described in Fig. 3.  $n$  and  $m$  are the numbers of corners and doors, respectively.  $\mathbf{P}_R$ ,  $\mathbf{P}_C$ , and  $\mathbf{P}_D$  represent the covariance matrices of the robot, all corners and doors, respectively, and  $\mathbf{P}_{RC}(\mathbf{P}_{CR})$ ,  $\mathbf{P}_{CD}(\mathbf{P}_{DC})$ , and  $\mathbf{P}_{RD}(\mathbf{P}_{DR})$  are the covariance matrices related to  $\mathbf{P}_R$  and  $\mathbf{P}_C$ ,  $\mathbf{P}_C$  and  $\mathbf{P}_D$ , and  $\mathbf{P}_R$  and  $\mathbf{P}_D$ , respectively.

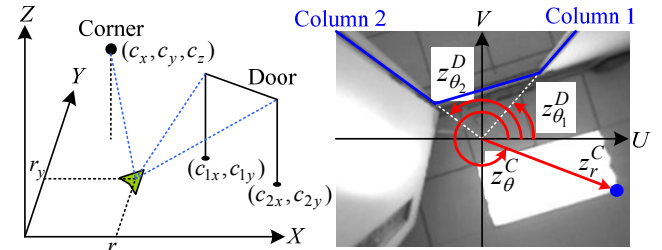


Fig. 3. Measurements in global and image coordinates.

The EKF algorithm based on Bayesian filtering (S. Thrun et al., 2005) consists of the prediction stage and update stage. At the prediction stage, the state vector  $\hat{\mathbf{X}}_k$  and its covariance matrix  $\mathbf{P}_k$  at time  $k$  are calculated from  $\hat{\mathbf{X}}_{k-1}$  and  $\mathbf{P}_{k-1}$  at time  $k-1$  and the encoder reading  $\mathbf{u}_k$  as follows:

$$\hat{\mathbf{X}}_k^- = f(\hat{\mathbf{X}}_{k-1}, \mathbf{u}_k) \quad (3)$$

$$\mathbf{P}_k^- = \nabla \mathbf{F}_x \mathbf{P}_{k-1} \nabla \mathbf{F}_x^T + \nabla \mathbf{F}_u \mathbf{Q} \nabla \mathbf{F}_u^T \quad (4)$$

where  $\mathbf{Q}$  represents the covariance matrix of the process noise,  $f$  is a function of the system dynamics, and  $\nabla \mathbf{F}_x = \partial f / \partial \mathbf{X}$  and  $\nabla \mathbf{F}_u = \partial f / \partial \mathbf{u}$  are the Jacobian matrices of the nonlinear function  $f$  with respect to the state and input, respectively. Note that the superscript “-“ indicates the state before the measurement at time  $k$  is taken.

If the robot sees the previously observed landmark, the EKF performs the update stage. The prediction of a landmark on the sensor frame, or the image coordinate, can be obtained by the following observation model based on the predicted system state.

$$\hat{\mathbf{Z}}_k = h(\hat{\mathbf{X}}_k^-) \quad (5)$$

where  $h$  represents the observation model used in this research. The observation models for the corners and doors are expressed by

$$\mathbf{Z} = [(\mathbf{z}_1^C)^T, \dots, (\mathbf{z}_n^C)^T, (\mathbf{z}_1^D)^T, \dots, (\mathbf{z}_m^D)^T]^T \quad (6)$$

$$\mathbf{z}^C = \begin{bmatrix} z_r^C \\ z_\theta^C \end{bmatrix} = \begin{bmatrix} \sqrt{(c_x - r_x)^2 + (c_y - r_y)^2} \times \frac{f_c}{c_z} \\ \frac{\pi}{2} - \tan^{-1} \frac{c_y - r_y}{c_x - r_x} + r_\theta \end{bmatrix} \quad (7)$$

$$\mathbf{z}^D = \begin{bmatrix} z_{\theta_1}^D \\ z_{\theta_2}^D \end{bmatrix} = \begin{bmatrix} \frac{\pi}{2} - \tan^{-1} \frac{c_{1y} - r_y}{c_{1x} - r_x} + r_\theta \\ \frac{\pi}{2} - \tan^{-1} \frac{c_{2y} - r_y}{c_{2x} - r_x} + r_\theta \end{bmatrix} \quad (8)$$

where  $f_c$  is the focal length of the camera,  $[z_r^C, z_\theta^C]^T$  and  $[z_{\theta_1}^D, z_{\theta_2}^D]^T$  denote the radius and angle of the corner and the angles of door columns in the polar coordinates as shown in Fig. 3, respectively (W. Y. Jeong et al., 2006). After observing the real features on the image, the measurement matrix  $\mathbf{Z}_k$  can be obtained, and the state vector and its covariance matrix  $\mathbf{P}$  at time  $k$  are updated as follows:

$$\hat{\mathbf{X}}_k = \hat{\mathbf{X}}_k^- + \mathbf{K}_k (\mathbf{Z}_k - \hat{\mathbf{Z}}_k) \quad (9)$$

$$\mathbf{P}_k = (\mathbf{I} - \mathbf{K}_k \mathbf{H}_k) \mathbf{P}_k^- \quad (10)$$

$$\mathbf{K}_k = \mathbf{P}_k^- \mathbf{H}_k^T (\mathbf{H}_k \mathbf{P}_k^- \mathbf{H}_k^T + \mathbf{V}_k \mathbf{R}_k \mathbf{V}_k^T)^{-1} \quad (11)$$

where  $\mathbf{K}$  represents the Kalman gain matrix,  $\mathbf{H} = \partial h / \partial \mathbf{X}$  and  $\mathbf{V} = \partial h / \partial \mathbf{v}$  are the Jacobian matrices of the observation model with respect to the state vector and the sensor noise, and  $\mathbf{R}$  is the covariance of the measurement noise.

### 3. DOOR CANDIDATE GENERATION

If a door feature is extracted reliably, it can be used as an important landmark in the EKF and the environment can be divided into the meaningful subareas using the detected doors. To detect a door, the vertical and horizontal lines can be exploited, which makes the matching process more robust than a corner feature because two vertical columns and one horizontal bar should be detected together from one door. However, in the real images, many vertical and horizontal lines can exist and detecting a door is a difficult task. In this research, several candidates are generated and evaluated to detect a door reliably.

#### 3.1 Obtaining candidates from vertical lines

When an upward camera sees the vertical lines perpendicular to the floor, these lines head toward the center of the image. This property can be used to extract the vertical lines of the door columns. To generate candidates for a door, it is necessary to group the neighboring vertical lines into a single line. Each group presents a candidate for a door column, and the candidates for a door are generated from these groups, as shown in Fig. 4. For  $n$  candidates for door columns,  $n(n-1)/2$  candidates for a door are generated. In this research, all lines are acquired by the Canny edge detection and Hough transform algorithms.

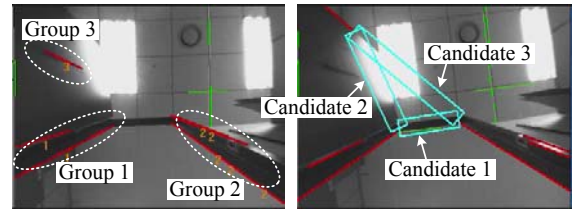


Fig. 4. Grouping of neighboring vertical lines (left), and all possible candidates (right). Rectangles represent the top of each candidate.

#### 3.2 Obtaining final candidates from horizontal lines

The final door candidates can be obtained by checking whether or not the horizontal lines exist between the vertical lines of the candidates obtained in section 3.1. Suppose the endpoint coordinates of the columns are found to be  $(p_{1u}, p_{1v})$  and  $(p_{2u}, p_{2v})$  in the image as a result of line extraction. However, these endpoints often differ from the actual ones due to the imperfection of line extraction. Therefore, the search area in which the horizontal lines can exist should be determined, as illustrated in Fig. 5(a). Provided that the robot is not located just below the door, the limit points  $(l_{1u}, l_{1v})$  and  $(l_{2u}, l_{2v})$  can be calculated by

$$\begin{aligned} l_{1u} &= d \cdot \cos \theta_1, \quad l_{1v} = d \cdot \sin \theta_1 \\ l_{2u} &= d \cdot \cos \theta_2, \quad l_{2v} = d \cdot \sin \theta_2 \\ d &= k \cdot f_c \cdot w / h_{\max} \end{aligned} \quad (12)$$

where  $\theta_1$  and  $\theta_2$  are the angles of the vertical lines on the image,  $k$  is a conversion factor from meter to pixel,  $w$  denotes the half width of the robot,  $h_{\max}$  denotes the maximum height of the door in the environment, and  $d$  represents the minimum distance from the horizontal line to the image center. Then, the range of the slope  $s$  of the horizontal line is defined by

$$\begin{aligned} s_1 &= \frac{p_{1v} - l_{2v}}{p_{1u} - l_{2u}}, \quad s_2 = \frac{p_{2v} - l_{1v}}{p_{2u} - l_{1u}} \\ \min(s_1, s_2) &< s < \max(s_1, s_2) \end{aligned} \quad (13)$$

Figure 5(b) is an example. If no horizontal line is extracted in the search area of a candidate, as shown in the upper figure of Fig. 5(b), this candidate is removed from the candidate set. In the lower figure of Fig. 5(b), however, a candidate which has a horizontal line in the search area is not removed and

considered a final candidate which will be evaluated in the next step (i.e., suitability test).

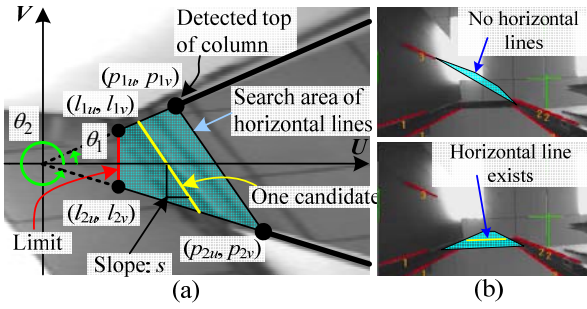


Fig. 5. (a) Search area of door horizontal lines, and (b) examples of candidate determination.

#### 4. SUITABILITY TEST

The set of candidates for a door can be obtained from not only an actual door but also other objects such as a wall or a bookshelf. Therefore, only an open door can be reliably detected using a monocular camera and exploited as a robust feature. Through the suitability test discussed below, the incorrect candidates can be removed and only the suitable door candidates which have the open area inside it are maintained. First, the position of a candidate is determined, and then the candidate will be checked whether it is an open door or not.

##### 4.1 Localization of candidates using particle filter

Before one candidate is convinced of being a suitable door, it cannot be applied directly to the EKF algorithm as a landmark. Therefore, every candidate should be evaluated whether it is suitable or not. To evaluate a candidate, the position of that candidate should be known, and in this research a particle filter is adopted to estimate the position of a door candidate.

Since the door used as a feature is stationary, its motion model need not be considered and only the update by the sensor model is useful. In Fig. 6, the fan-shaped area represents the uncertainty of observation, and its center line shows the direction of measurement.  $\theta_{error}$ ,  $\alpha_{error}$  and  $\beta_{error}$  mean the maximum errors of each measurement. The samples are weighted by the three importance factors ( $w_\theta$ ,  $w_\alpha$ , and  $w_\beta$ ) which are affected by three angle errors ( $\theta$ ,  $\alpha$ , and  $\beta$ ) respectively. Then, the resulting weights of samples are reflected in the next step, re-sampling, to make samples converge near the actual position of a door. A triangular distribution is adopted for the sensor model to reduce the computational burden.

To estimate the position of one candidate, 200 random samples are drawn in the 3D space in Fig. 7(a). As the robot moves in Fig. 7(b), the initially distributed samples converge according to the probabilities of samples updated by the sensor model of Fig. 6. In Fig. 7(c), the samples converge to one position through sufficient observations, and therefore the positions of two columns are obtained from the mean value of the converged samples.

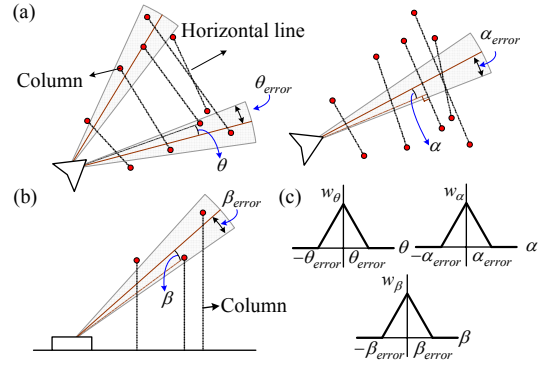


Fig. 6. Sensor models for door detection; (a) top view, (b) side view, and (c) importance factors.

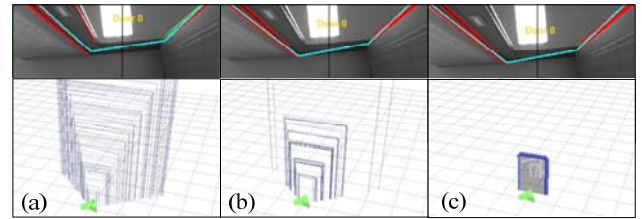


Fig. 7. Estimation of candidate position using particle filter.

##### 4.2 Edge projection onto virtual plane

Some candidates may contain other objects such as a bookshelf or a poster on the wall since these objects also have vertical and horizontal lines. After estimating the position of a candidate, all edges within that candidate on the image are assumed to be extracted from the surface of a closed door or a wall. The plane which includes this surface will be called a “virtual plane.” This virtual plane perpendicular to the floor can be calculated using the positions of two columns ( $c_{1x}$ ,  $c_{1y}$ ) and ( $c_{2x}$ ,  $c_{2y}$ ). The relationship between the shape of the door on the image and the virtual plane is illustrated in Fig. 8.

A normal vector  $\mathbf{n} = (n_x, n_y, n_z)$  can be determined by

$$\begin{bmatrix} n_x \\ n_y \\ n_z \end{bmatrix} = \begin{bmatrix} \cos(\pi/2) & \sin(\pi/2) & 0 \\ -\sin(\pi/2) & \cos(\pi/2) & 0 \\ 0 & 0 & 1 \end{bmatrix} \begin{bmatrix} c_{1x} - c_{2x} \\ c_{1y} - c_{2y} \\ 0 \end{bmatrix} \quad (14)$$

$$= \begin{bmatrix} c_{1y} - c_{2y} \\ c_{2x} - c_{1x} \\ 0 \end{bmatrix}$$

Hence, the equation of the virtual plane is

$$n_x(x - c_{1x}) + n_y(y - c_{1y}) + n_z z = 0 \quad (15)$$

When a robot moves, a point ( $q_u$ ,  $q_v$ ) which is considered a point on the surface of a door or a wall is continuously projected onto the virtual plane as shown in Fig. 9(a). To obtain the projected point ( $q_x$ ,  $q_y$ ,  $q_z$ ) in 3D space, a direction vector  $\mathbf{d} = (d_x, d_y, d_z)$  from the robot to the point ( $q_x$ ,  $q_y$ ,  $q_z$ ) is calculated by

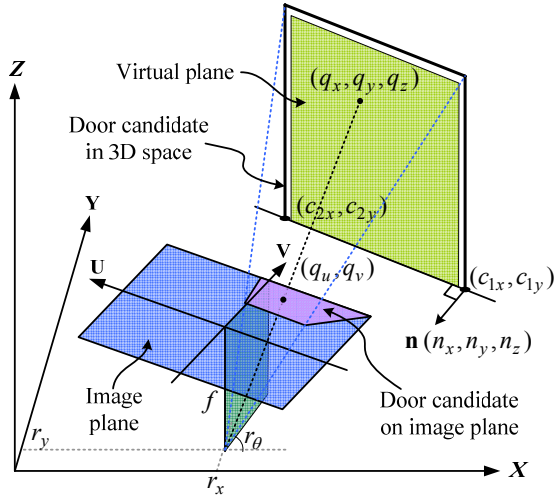


Fig. 8. Geometric relationship between image plane and virtual plane.

$$\begin{bmatrix} d_x \\ d_y \\ d_z \end{bmatrix} = \begin{bmatrix} q_v \cos r_\theta - q_u \sin r_\theta \\ q_v \sin r_\theta + q_u \cos r_\theta \\ f_c \end{bmatrix} \quad (16)$$

The point  $(q_x, q_y, q_z)$  on the virtual plane is located at the end-point of the vector  $t \cdot \mathbf{d}$  from the position of the robot with a real number  $t$ . Finally, using (15) and (16), the projected point  $(q_x, q_y, q_z)$  is calculated by

$$\begin{bmatrix} q_x \\ q_y \\ q_z \end{bmatrix} = t \cdot \begin{bmatrix} d_x \\ d_y \\ d_z \end{bmatrix} + \begin{bmatrix} r_x \\ r_y \\ 0 \end{bmatrix} \quad (17)$$

$$t = -\frac{n_x(r_x - c_{1x}) + n_y(r_y - c_{1y})}{n_x d_x + n_y d_y}$$

The projected edge points on the virtual plane calculated by (17) are maintained until the whole process of the suitability test ends. These points are projected on the image plane during the test and continuously compared to the newly detected edge points.

To compare these two edge point sets, a Hausdorff distance (HD) and modified Hausdorff distance (MHD) is measured. HD is compatible for the object matching in the image processing field (M.P. Dubuisson et al., 1994). Let  $A = \{a_1, \dots, a_{N_a}\}$  denotes the edge points projected on the image plane from the virtual plane and  $B = \{b_1, \dots, b_{N_b}\}$  denotes newly extracted edge points from the camera image. Then the HD,  $H(A, B)$ , and MHD,  $h_{mod}(A, B)$ , between two edge sets  $A$  and  $B$  are defined by

$$H(A, B) = \max(h_{mod}(A, B), h_{mod}(B, A)), \quad (18)$$

$$h_{mod}(A, B) = \frac{1}{N_a} \sum_{a \in A} \min_{b \in B} \|a - b\|.$$

When the candidate is extracted on the closed object like a poster on the wall as shown in Fig. 9(a), there is no difference between these two edge point sets as the robot moves. In the case of Fig. 9(b), the HD becomes larger as the robot moves,

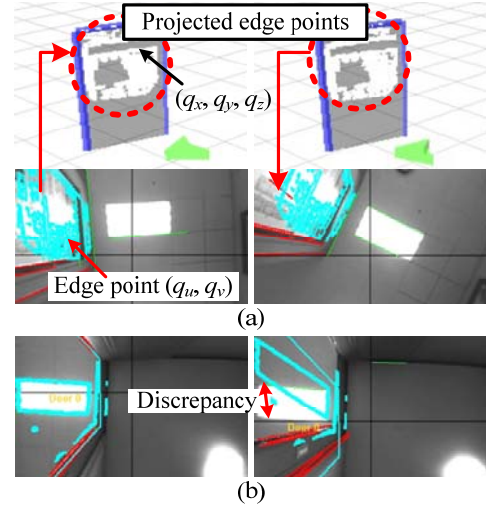


Fig. 9. Projection of edges; (a) closed, and (b) open doors.

and if this value exceeds the threshold, it is determined that the area is open. Thus, whether one candidate is open or not can be determined by HD, and then an open door is registered to the EKF as a landmark.

## 5. RESULTS

Several experiments were conducted in the real environment using the ActivMedia Pioneer 3-DX robot equipped with an upward camera and a laser scanner. The calibrated image was acquired by the CMOS camera with a field of view of 130°. A grid map with cells of 10cm x 10cm was built by a laser scanner. The size of the experimental environment was 8m x 10m which included two doors inside, as shown in Fig. 10. The SLAM process used the corners extracted by the Harris corner detector and the doors detected by the proposed method. The unstable features were autonomously deleted. The whole process of the proposed algorithm worked in real-time in a notebook computer with a 1.83 GHz CPU.

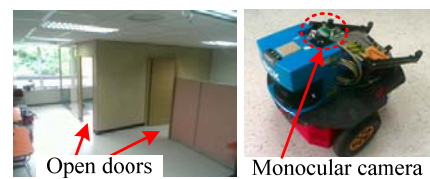


Fig. 10. Experimental environment and platform.

Figure 11 shows the experimental results. The ellipsoids represent the covariance of the corners. The robot started to perform SLAM using the corners in the unknown environment in Fig. 11(a). The elements of a door were detected in Fig. 11(b), and then a set of door candidates were generated. The particle filter determines the shape and position of the door in Fig. 11(c). Note that one unstable feature in Fig. 11(b) was deleted in Fig. 11(c). If the wrong candidates were generated from the wall or furniture, the algorithm checked their suitability and deleted them from the candidate set in Fig. 11(d). The second door was detected and registered in Fig. 11(e) and (f), and finally all the unstable features were deleted. The grid map was successfully built by the proposed monocular SLAM because the localization error

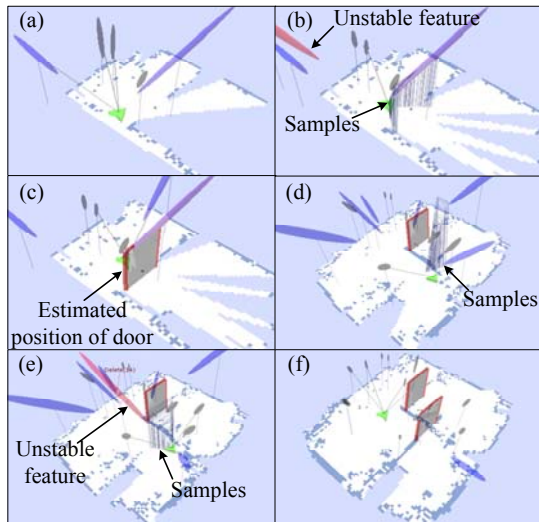


Fig. 11. Indoor monocular SLAM with corners and doors.

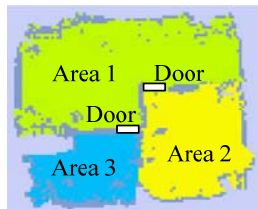


Fig. 12. Division of environment using doors.

mainly due to the slippage between the robot and the floor was corrected well.

The doors can divide indoor environments such as a kitchen, a corridor, or an office into several sub-areas. Therefore, the grid map can be partitioned into several parts using the doors detected, as shown in the example in Fig. 12. These divided areas can be considered each individual space, and the pose estimation such as the EKF can separately work to reduce the computational burden and cover the large environment.

## 6. CONCLUSIONS

In this paper, the door which is one of the most useful features in an indoor environment is detected using the lines extracted by an upward monocular camera. A door can be used as a feature for SLAM, and it can also serve to divide the environment into the meaningful areas. The SLAM algorithm based on this proposed door detection scheme was validated by several experiments. From this research, the following conclusions have been drawn.

1. A door can be reliably detected using the lines through the candidate generation and suitability test, although many vertical and horizontal lines are extracted from the image of the real environment.
2. Since both corner and door features are used together in this research, the proposed SLAM method can work more robustly in the various environments than the previous SLAM methods that use only corner features.
3. The environment can be divided into several meaningful areas using the detected doors during SLAM.

## ACKNOWLEDGEMENT

This paper was performed for the Intelligent Robotics Development Program, one of the 21st Century Frontier R&D Programs funded by the Ministry of Commerce, Industry and Energy of Korea.

## REFERENCES

- A. Davison (2003). Real-time simultaneous localisation and mapping with a single camera. *Proc. of the ninth Int. Conf. on Computer Vision*. pp. 1403-1410.
- D. Anguelov, D. Koller, E. Parker, and S. Thrun (2004). *Proc. of the IEEE Int. Conf. on Robotics and Automation*. pp. 3777-3784.
- G. Jang, J. Kim, S. Kim, and I. Kweon (2005). PR-SLAM in particle filter framework. *Proc. of the IEEE Int. Symposium on Computational Intelligence in Robotics and Automation*. pp. 327-333.
- J. Folkesson, P. Jensfelt, and H. I. Christensen (2005). Visual SLAM in the measurement subspace. *Proc. of the IEEE Int. Conf. on Robotics and Automation*. pp. 30-35.
- M.P. Dubuisson and A.K. Jain (1994). A modified Hausdorff distance for object matching. *Proc. of the 12th IAPR Int. Conf. on Pattern Recognition*. pp. 566-568.
- P. Smith, I. Reid, and A. Davison (2006). Real-time monocular SLAM with straight lines. *Proc. of BMVC06*.
- S. Thrun, W. Burgard and D. Fox (2005). *Probabilistic Robotics*. MIT Press.
- W. Y. Jeong and K. M. Lee (2006). Visual SLAM with line and corner features. *Proc. of the IEEE/RSJ Int. Conf. on Intelligent Robots and Systems*. pp. 2570-2575.